NANO LETTERS

pubs.acs.org/NanoLett Letter

Unexpected Near-Infrared to Visible Nonlinear Optical Properties from 2-D Polar Metals

Megan A. Steves, Yuanxi Wang, Natalie Briggs, Tian Zhao, Hesham El-Sherif, Brian M. Bersch, Shruti Subramanian, Chengye Dong, Timothy Bowen, Ana De La Fuente Duran, Katharina Nisi, Margaux Lassaunière, Ursula Wurstbauer, Nabil D. Bassim, Jose Fonseca, Jeremy T. Robinson, Vincent H. Crespi, Joshua Robinson, and Kenneth L. Knappenberger Jr*

Cite This: https://dx.doi.org/10.1021/acs.nanolett.0c03481 Read Online

ACCESS | Metrics & More | Article Recommendations | Supporting Information

ABSTRACT: Near-infrared-to-visible second harmonic generation from air-stable two-dimensional polar gallium and indium metals is described. The photonic properties of 2D metals, including the largest second-order susceptibilities reported for metals (approaching 10 nm/V), are determined by the atomic-level structure and bonding of two-to-three-atom-thick crystalline films. The bond character evolved from covalent to metallic over a few atomic layers, changing the out-of-plane metal−metal bond distances by approximately ten percent (0.2 Å), resulting in symmetry breaking and an axial electrostatic dipole that mediated the large nonlinear response. Two different orientations of the crystalline metal atoms, corresponding to lateral displacements <2 Å, persisted in separate micrometer-scale terraces to generate distinct harmonic polarizations. This strong atomic-level structure−property interplay suggests metal photonic properties can be controlled with atomic precision.

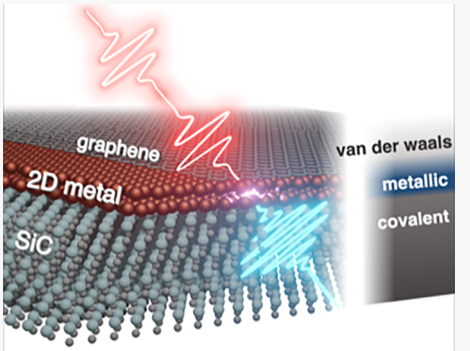

KEYWORDS: *2D materials, 2D metals, second harmonic generation, polar metals, confinement heteroepitaxy, nonlinear photonics*

Nonlinear frequency mixing (e.g., harmonic generation) and polarization rotation of electromagnetic waves are the foundation of many important and emergent applications, including laser technologies, optical switches, chemical sensing, telecommunications, and frequency combs, among others.[1] The current state-of-the-art method for second-order harmonic generation is achieved using a sequence of multiple quantum wells that are designed to enhance transitions resonantly at both fundamental and harmonic frequencies.[2] However, these systems are intrinsically limited to the mid-infrared, precluding their operation at frequencies relevant for telecommunications, or where the resolution of molecular or biological imaging can be significantly enhanced. Therefore, strategies for achieving large nonlinear optical responses over a broader range of frequencies are needed. Although emerging two-dimensional semiconductors have shown great potential for nonlinear optical performance at higher frequencies, the reported second-order susceptibilities $\chi^{(2)}$ of these systems remain orders of magnitude smaller than those of multiple quantum wells.[2−10]

Owing to their strong, broadband electromagnetic interactions, nanostructured metals offer the potential to establish a new state-of-the-art method, in the visible and near-infrared, for nonlinear optical transduction. Achieving this new standard will require a predictive understanding of the interplay between material structure and nonlinear optical response. However, metal structure−property correlations outside of vacuum have been primarily limited to gold. Here, we report extremely efficient second harmonic generation from air-stable 2D metal heterostructures, with room-temperature near-infrared $\chi^{(2)}$ values approaching 10 nm/V. This extraordinary nonlinear response was obtained from a heterostructure consisting of crystalline, atomically thin group-IIIa metal films (gallium or indium) that are epitaxial to a SiC substrate and capped *in situ* with graphene. The metal films extend over several hundred square micrometers adopting the hexagonal lattice of SiC, but the surprisingly large $\chi^{(2)}$ values are the result of subtle structural effects that occur on the atomic scale, which lead to axial symmetry breaking that is unique to the composite heterostructure—a hexagonal metal is not expected to yield large in-plane second-order responses. This symmetry breaking, combined with quantum-confined electronic interband transitions resonant with the laser fundamental, results in the large in-plane $\chi^{(2)}$. The bonding character of the metal evolves from predominately covalent at the SiC/metal interface to primarily metallic between metal layers and to nonbonded

Received: August 27, 2020
Revised: October 6, 2020

https://dx.doi.org/10.1021/acs.nanolett.0c03481
Nano Lett. XXXX, XXX, XXX−XXX

(van der Waals-like) at the metal/graphene interface, as reflected in an ∼10% variation in the metal's layer-to-layer spacing (for three-layer gallium) along with an electrostatic gradient over two (indium) or three (gallium) atomic layers. This asymmetry leads to a theoretically predicted axial dipole and out-of-plane $\chi^{(2)}$ that is confirmed by angle-dependent second harmonic generation (SHG) measurements, verifying that these are 2D polar metals (2D-PMets). Density functional theory (DFT) calculations predict in-plane and out-of-plane second-order susceptibilities consistent with experimental measurements, as well as the presence of visible-to-near-infrared electronic interband resonances, which may be leveraged to further amplify the intrinsically large nonlinear response of 2D-PMets.

In addition to efficient NLO transduction, polarization modulation is essential for efficient nonlinear optical switching. Correlative electron and polarization-dependent SHG microscopy resolves structural influences of the SiC substrate that are persistent into the metals and influence their far-field photonic properties. Specifically, we show that angstrom-level defects, such as step edges, cause alternations in the metal film structure that extend for micrometers. As a result, spatially periodic recurrences of polarization-dependent NLO signals were observed. Taken together, these structural and optical analyses indicate that the efficient $\chi^{(2)}$ and polarization-dependent responses of the 2D polar metals are determined at the atomic level. Hence, control over interfacial bonding and structure may provide opportunities for further breakthroughs in room-temperature visible-to-near-infrared nonlinear optical technology that can be tailored at the atomic level using nonprecious metals.

Two-dimensional Ga and In layers are formed through a process called confinement heteroepitaxy (CHet), where metal atoms intercalate to the interface between epitaxial graphene and SiC, forming crystalline 2D metals registered to the SiC.[11] The native interface of epitaxial graphene on SiC contains dangling bonds which may be readily passivated through intercalation of metal atoms. The graphene layers not only aid in stabilizing the 2D metal films but also protect against oxidation, as confirmed in previous X-ray photoelectron spectroscopy studies.[11] Cross-sectional scanning transmission electron microscopy (STEM) verifies that intercalation at the SiC/graphene interface yields crystalline metals 2−3 atomic layers thick, consistent with DFT phase stability calculations.[11] Using a 2D-Ga prototype (Figure 1a), calculated charge densities indicate that the first Ga layer bonds covalently with the SiC substrate; the bonding character then evolves to interlayer metallic bonding and finally to van der Waals interactions (with weak charge transfer) between the top Ga layer and graphene.[11] This depth-dependent evolution in bonding character induces out-of-plane symmetry breaking throughout the metal layer, yielding a 2D polar metal (2D-PMet) with an intrinsic axial dipole. Importantly, the hermetic seal created by the graphene overlayer enables extensive ex-situ characterization of the 2D-PMet without degradation of the metal.[11]

Owing to the breaking of inversion symmetry by this out-of-plane atomic-level structure, 2D-PMets can function as strong second-order nonlinear optical transducers. This is evidenced by NLO spectra investigated through SHG imaging. Figure 1b compares NLO spectra for 2D-In and 2D- Ga to (i) a 2.5 nm-thick Au film on SiC encapsulated with CVD graphene (SI Methods) and (ii) 3D gold nanorods, which are standard

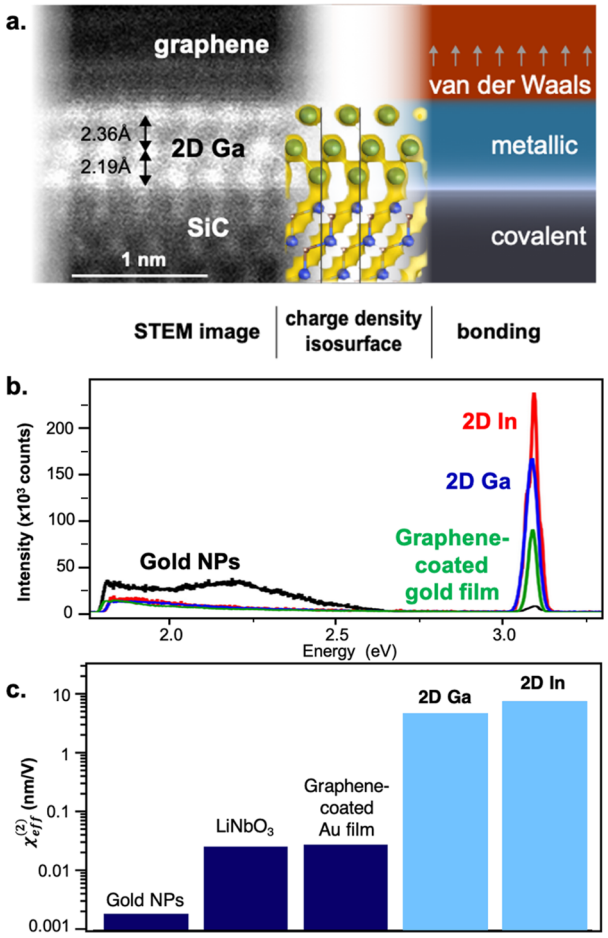

Figure 1. Structure and nonlinear optical properties of 2D-PMets. (a) Cross-sectional STEM images reveal the layers of the SiC substrate/2D Ga/bilayer graphene structure, which shows a 10% change in metal lattice parameters between layers (left). An evolution of bonding character is present (right), resulting in an electrostatic gradient conveyed by the computed charge-density isosurface (center). (b) Nonlinear spectra for 2D-PMets and 3D gold nanoparticles, demonstrating the enhanced SHG/TPPL ratio of 2D metals. (c) Comparison of $\chi^{(2)}$ values for 2D-PMets and other materials. All reported values are calculated using the average power of the fundamental.

metallic nanostructures for investigating NLO response.[12] 2D-PMets are characterized by prominent NLO peaks at 3.1 eV, resulting from SHG of the 1.55 eV fundamental, which was confirmed from quadratic signal power dependences (Figure S1A). In contrast, the NLO spectra of three-dimensional gold nanorods are dominated by broad two-photon photoluminescence typical of colloidal coinage metals[13] with a minor contribution from SHG. Based on a polarizable sheet model (SI Methods), the integrated intensities of the experimentally measured SHG were used to calculate the magnitudes of the per-volume second-order susceptibility $\chi^{(2)}$ for these systems, which are compared in Figure 1c.[14] Comparison of NLO performance of emerging 2D materials depends on the model used to convert experimentally measured SHG intensities to a quantifiable second-order susceptibility. Because of the two-dimensional nature of PMets, we model the system as a nonlinear polarizable sheet to avoid potential overestimations of the nonlinear susceptibility, which can result from the use of bulk models.[10,15] For 2D-PMets, values of 4.6 ± 0.7 and 8.5 ±

https://dx.doi.org/10.1021/acs.nanolett.0c03481
Nano Lett. XXXX, XXX, XXX−XXX

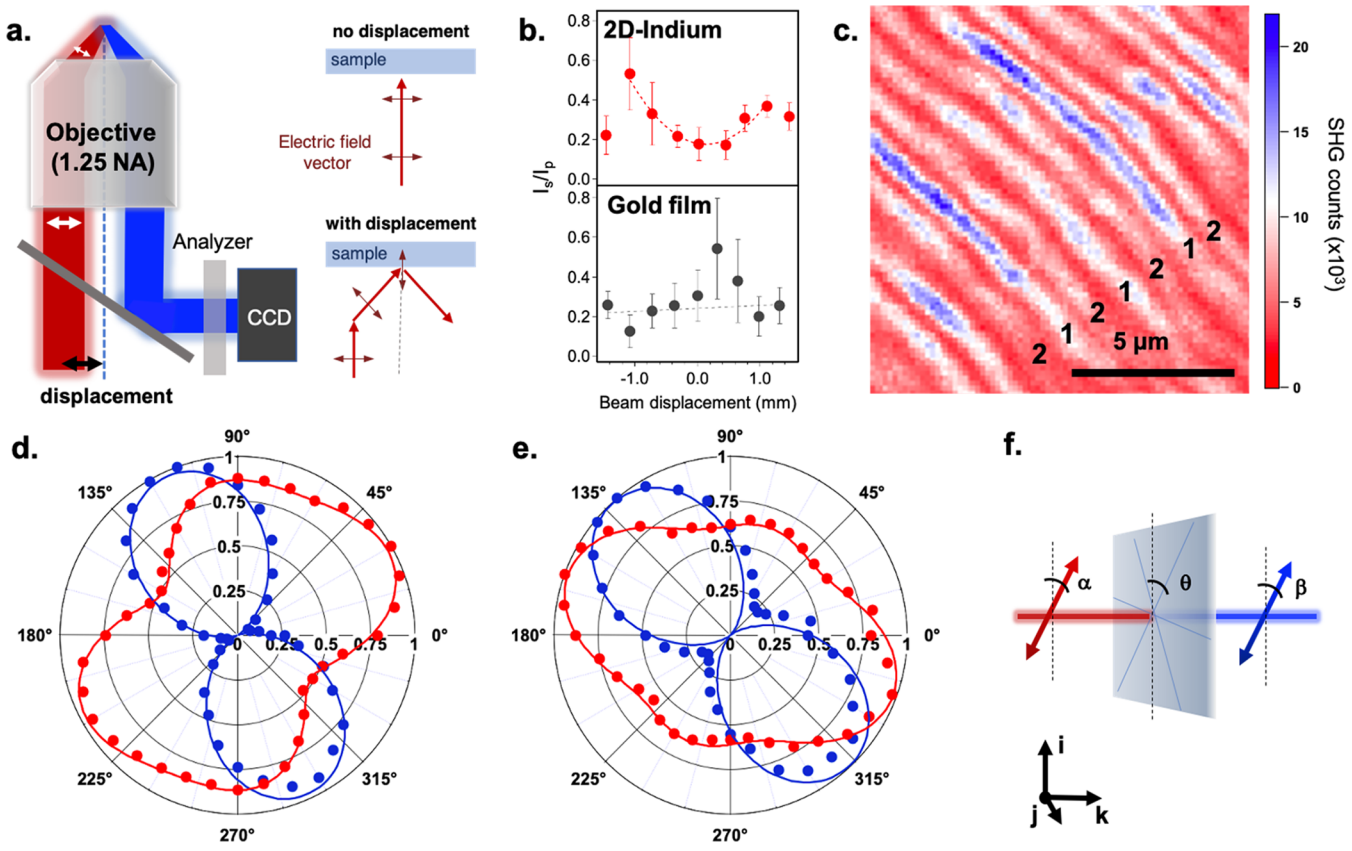

Figure 2. Probing the structure of 2D-In using angle- and polarization-resolved SHG microscopy. (a) Experimental setup for angle-resolved SHG measurements used to obtain (b) the ratio of I_p/I_s for one type of stripes as a function of beam displacement. The dashed line is a guide illustrating the approximate quadratic dependence of the data. Results for a gold film are shown for comparison. (c) Example SHG-detected image of 2D-In. Distinct regions, labeled 1 and 2, demonstrate different polarization responses. (d, e) Representative examples of excitation (red) and emission (blue) polarization-dependent SHG intensities obtained by changing α and β, respectively, for Type 1 (d) and Type 2 (e) regions. Filled circles show the experimental data, while the dashed lines are fits to the data using the parameters in Table S1. (f) Schematic of polarization-resolved experimental setup, depicting the angles used in the polarization analysis. The angle of the crystal axis with respect to the laboratory $\hat{i}$ axis is given as θ. Variables α and β are the polarization of the fundamental and harmonic waves, respectively, within the sample plane and are referenced to the $\hat{i}$ axis.

0.6 nm/V are obtained for 2D-Ga and 2D-In, respectively. These values are calculated using metal thicknesses of 0.60 and 0.45 nm, as estimated from cross-sectional STEM.[11] While SiC and epitaxial graphene also exhibit nonlinear signal, the SHG yield from graphene/SiC is small compared to that from a 2D-PMet-based heterostructure. Both 2D-PMets show $\chi^{(2)}$ values more than 1000× those of 3D gold nanorods and over 100× larger than graphene-coated Au films and industrial standards such as $LiNbO_3$.[14] Because $\chi^{(2)}$ values are intrinsically higher for lower bandgap materials,[16] we also compare the 2D-PMets to other metal-surface SHG sources using per-area units (nm^2/V).[17,18] The in-plane components of 2D-Ga and 2D-In are $\chi^{(2)}_{yyy}$ = 4.8 and 3.8 nm^2/V, respectively, which is reasonably consistent with DFT ($\chi^{(2)}_{yyy}$ = 3 nm^2/V for 2D In, see SI Methods). Furthermore, 2D-PMets are predicted to be more efficient than other metal-surface SHG sources like Al(111), which is theoretically estimated to have a $\chi^{(2)}_{yyy}$ of 0.2 nm^2/V.[19] Hence, the Ga and In 2D-PMets exhibit the largest χ^2 reported for any metal transducer.

With the extra-ordinarily efficient nonlinear optical response of 2D-PMets established, we next confirm the importance of their out-of-plane symmetry breaking in producing the surprisingly large $\chi^{(2)}$ values. Since centrosymmetric crystals have zero $\chi^{(2)}$, bulk Ga and In with D_{2h} (mmm) and D_{4h} (4/mmm) point group symmetries (crystal classes), respectively, are not expected to generate SHG. Even considering a hypothetical freestanding 2D metal with hexagonal packing as imposed by the SiC substrate, two and three atomic layers with AB and ABC stacking belong to the C_{6h} point group, which is centrosymmetric and thus not SHG-active. The actual inversion symmetry breaking of the 2D-PMets relies on the out-of-plane polarity, as verified using the angular dependence of the p- and s-polarized SHG intensities (I_p/I_s). The electric field of the fundamental is aligned with the axial dipole by internal reflection at the sample plane using the objective by beam translation parallel to the polarization vector (Figure 2a). If an axial dipole is present, the SHG ratio $I_p(2\omega)/I_s(2\omega)$ is expected to increase quadratically with increasing beam displacement from the center of the objective back aperture.[20] Figure 2b, which portrays the angular dependence of one of the striped regions from Figure 2c (discussed below), demonstrates this to be the case. In contrast, no angular dependence was detected for 5 nm thick gold films encapsulated with graphene because its out-of-plane $\chi^{(2)}_{zzz}$ is similar in magnitude to its in-plane $\chi^{(2)}_{yyy}$.[17] We note that internal reflection is achieved in our microscope at beam displacements of ±0.8 mm; hence, further displacement reduced I_s/I_p (SI). The axial dipole revealed by the Figure

https://dx.doi.org/10.1021/acs.nanolett.0c03481
Nano Lett. XXXX, XXX, XXX−XXX

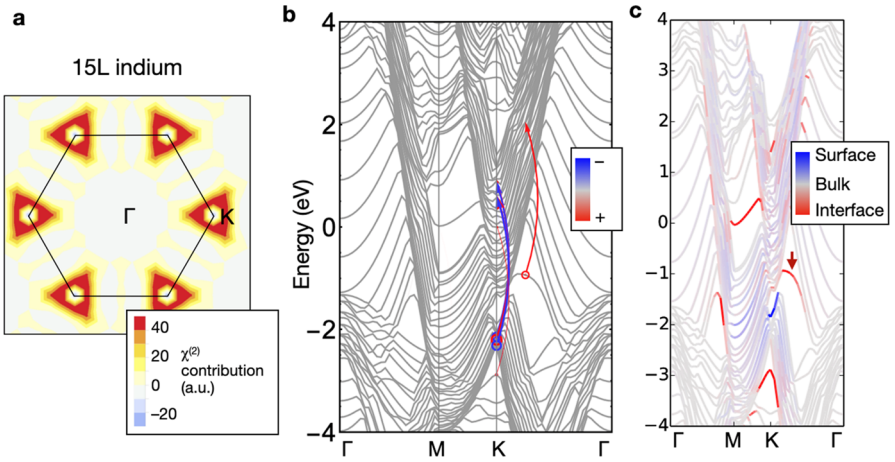

Figure 3. (a) Reciprocal space decomposition of $\chi^{(2)}$ for a hypothetical 15L-In/SiC within $\omega = 1.5 \pm 0.2$ eV. Dominant contributions appear close to K. (b) Further decomposition by bands, showing only the dominant transitions at 2ω, with signs indicated by red or blue. (c) Same band structure but with red and blue colors indicating projection onto atomic orbitals of In atoms at the metal/SiC interface and at the surface.

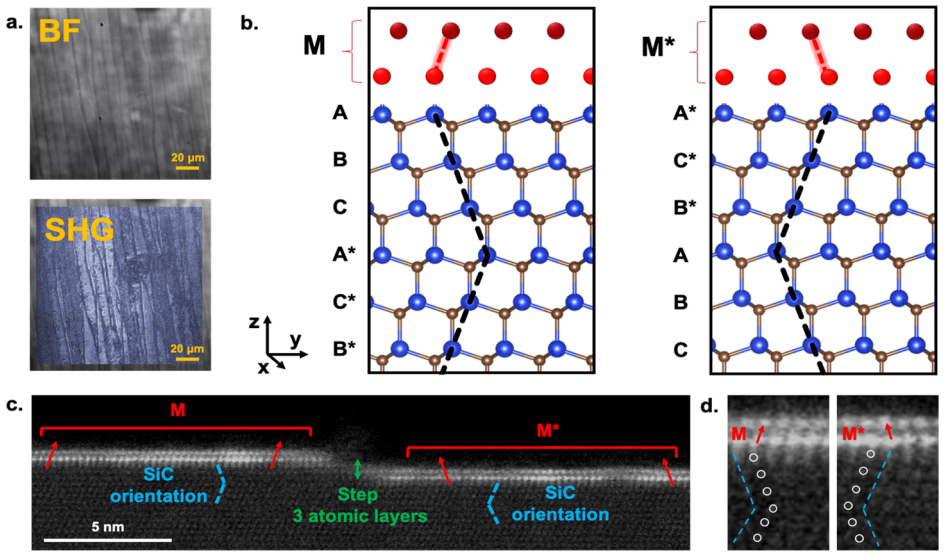

Figure 4. Structural origin of the stripes observed in polarization-resolved SHG. (a) Correlative brightfield (top) and SHG (bottom) imaging demonstrating that step edges separate different regions. (b) Schematic depicting the In (red) orientations M and M*, where the first layer of In is epitaxial to the silicon (blue) and the second layer is registered over the uppermost carbon (brown) atoms. (c) STEM image of 2D-In cross-section, demonstrating the change from M to M* orientation at a SiC step edge. (d) Larger view of two areas selected from panel c focusing on the M and M* orientations. Circles indicating the approximate location of Si atoms and dashed lines are added as a guide to the eye.

2b data is thus a distinct feature of the CHet-formed 2D-PMets, one that is likely associated with the strong layer-by-layer gradient in bonding character and results in efficient second-order nonlinear optical transduction.

The intrinsically large $\chi^{(2)}$ of the polar metals is enhanced by interfacial electronic states that resonate at the fundamental frequency. The localization of these states to the metal/SiC interface is demonstrated by decomposition analysis of $\chi^{(2)}_{yyy}$ for hypothetical thicker layers of metals on SiC, where interface, surface, or bulk contributions can be unambiguously distinguished spatially. Using 2D-In as a prototypical 2D-PMet, we first decompose $\chi^{(2)}_{yyy}$ for a 15-layer indium/SiC in reciprocal space (Figure 3a) for $\omega = 1.5 \pm 0.2$ eV, where dominant contributions appear close to K. These near-K transitions are more clearly identified when further decomposed by bands in Figure 3b, connecting states from −1 to 2 eV by 2ω; other strong transitions from lower-energy bulk bands at exactly K do not add constructively to a significant summed contribution, as indicated by their incoherent signs (color-coded in red and blue; see Supporting Information for additional details). A final comparison of Figure 3b with the atomic-orbital-projected band structure in Figure 3c reveals that the initial state of the dominating near-K transition is indeed localized at interfacial In and Si atoms. Owing to their atomic-level geometric and electronic structure, the $\chi^{(2)}$ of 2D-PMets are, to our knowledge, the largest reported for metallic transducers and may provide a platform for achieving near-infrared second-order responses that can compete favorably with the impressive mid-infrared values obtained for multiple-quantum-well structures.[2,9]

NLO transduction by these metals may be further enhanced by resonant electronic excitation such as visible-to-near-infrared interband excitations (Figure S4).[21] Additionally, 2D-PMets are theoretically predicted to support plasmon resonances at specific frequencies throughout the visible and near-infrared frequency ranges (Figure S5). Hence, the SHG

https://dx.doi.org/10.1021/acs.nanolett.0c03481
Nano Lett. XXXX, XXX, XXX−XXX

response may also be increased by local surface fields.[22,23] Thus, several avenues for further amplification of 2D-PMet nonlinear responses by resonance matching with the fundamental (ω) or harmonic (2ω) frequencies exist. Moreover, the atomic thickness of 2D-PMets leads to quantized resonances that can be used to form hybrid resonances in multicomponent heterojunctions. These quantized hybrid states could be leveraged to mediate efficient nonlinear optical processes at wavelengths important to telecommunications and optoelectronic applications.

Next, the influence of the in-plane 2D-PMet structure on second harmonic generation is described. The substrate is a dominant factor in determining the interfacial structure and, in turn, the optical response of the 2D-PMet. Beyond the large $\chi^{(2)}$ values, this influence is responsible for the formation of polarization-dependent SHG signals. This behavior is portrayed in Figure 2C, where two types of regions with distinct polarization patterns are detected in 2D-In. The two regions, which have similar maximum SHG intensities, alternate spatially in striped patterns (labeled 1 and 2), with distinct SHG-intensity polarization dependences (Figure 2d,e and Movies S1 and S2). Analysis of these polarization patterns in terms of a rank-three nonlinear susceptibility tensor (SI Methods) provides evidence for the origin of the striping. The polarization and crystal axes are defined with respect to the lab frame in Figure 2f, with θ being the angle of the 2D-PMet crystal axis with respect to the sample plane and α and β the polarization angles of the fundamental and harmonic within the sample plane. Fitting the SHG excitation and emission polarization patterns (Figure 2d,e) retrieves both θ and the relative magnitudes of each element of the nonlinear susceptibility tensor for each stripe type (SI Methods). Compared to the expectations for the major crystal classes, the $\chi^{(2)}$ elements obtained by fitting (Table S1) most closely match a polar C_{3v} (3m) point group symmetry for both types, but with moderate deviations resulting from defects. This correspondence with the C_{3v} structure provides further evidence that the 2D-In is polar and adopts the in-plane symmetry of the SiC substrate. Similar polarization dependences are observed in 2D-Ga (Figure S1b,c), which implies that substrate templating of the metal is a general phenomenon.

Correlated bright-field and SHG microscopy demonstrate that the stripe regions are separated by step edges in the SiC substrate (Figure 4a). Comparison of optical and atomic force microscopy images also support this interpretation, indicating that the observed SHG stripes result from metal terraces that persist for several micrometers (Figure S2). Cross-sectional STEM analysis confirms that the sample in Figure 2a is predominantly two atomic layers of In (Figure S3). While some areas with other thicknesses are observed, these are not correlated with SiC steps, and hence, we rule out differences in metal thickness as the cause of the alternating polarization patterns. On the other hand, 6H-SiC is known to alternate its layer stacking order every three SiC units (Figure 4b). Taken together with the registry of the first- and second-layer metal atoms above the uppermost Si and C atoms, respectively (Figures 1 and S3), we infer that the structural alternation in the SiC substrate results in a metal lattice rotation of 180° at every three-unit-high step in the SiC substrate. The result is two possible metal orientations relative to the first layer of carbon in the SiC substrate, which we label M and M*, which have the in-plane nonlinear susceptibility elements

$$\begin{pmatrix} yxx & yyy & xxy \end{pmatrix} = \begin{pmatrix} -1+n & 1 & -1+n \end{pmatrix}_{M} \text{ and } \begin{pmatrix} 1+n & -1 & 1+n \end{pmatrix}_{M^*}$$

where n represents deviations from C_{3v} symmetry caused by defects (for example, 1D-step edges along $(1\bar{1}0n)$ SiC). Inspection of the $\chi^{(2)}$ elements obtained from fitting of the polarization patterns of 2D-PMets for type 1 and 2 stripes reveals them to be consistent with this model and allows us to observe that the contribution from defects is consistent with C_{1h} symmetry. Thus, we conclude that alternating metal orientations combined with in-plane symmetry-breaking defects cause the distinguishable striped regions observed with polarization-resolved SHG microscopy. We also directly observe the inversion of metal orientation at a step edge through STEM imaging of 2D-In (Figure 4c). Taken together, correlative polarization-resolved and angle-dependent SHG and electron microscopy, along with theoretical calculations, implicate unique roles for out-of-plane and in-plane symmetry breaking for determining the optical responses of the 2D-PMets; whereas the out-of-plane structure is fundamental to the large SHG signals, in-plane symmetry breaking determines their distinct polarization response. Although the interfacial structure determined the SHG polarization response, the $\chi^{(2)}$ values were uniform across the 2D-PMet. This observation implies that synthetic control over the lattice properties could lead to efficient polarization-selective nonlinear optical properties of 2D metals.

The results presented here indicate that 2D polar metals formed by confinement heteroepitaxy could provide a materials platform for unprecedented nonlinear optical transduction at the technologically important visible-to-near-infrared frequency range. Moreover, we find that the surprising nonlinear optical properties of these systems result from their unique bonding and lattice properties, which are determined with structural precision on the atomic level. These angstrom-scale effects extend uniformly through the metals on a micrometer length scale, providing rich second-order nonlinear optical properties. Because the SiC-metal interaction determines both the in-plane and out-of-plane symmetry of 2D-PMets, there is strong potential for tuning material nonlinear susceptibilities (e.g., $\chi^{(2)}$) by controlling substrate−metal interactions, and the air stability of the CHet platform (through graphene encapsulation) means that many metals beyond Au are now candidates for study, optimization, and utilization of NLO response. The SHG polarization and angular dependences observed here are unique to the atomic-level interfacial structure of the 2D polar metals. Hence, 2D-PMets may have intrinsic advantages for optical switching applications and for forming nonlinear metasurfaces. In particular, defects were shown to induce lateral metal atom displacements of <2 Å that persisted in terraces for several micrometers. These subtle structural differences resulted in the generation of harmonic signals with distinct polarizations. Therefore, structural changes at the atomic level may serve as a template for controlling the lattice and photonic properties of metals.

■ ASSOCIATED CONTENT

Supporting Information

The Supporting Information is available free of charge at https://pubs.acs.org/doi/10.1021/acs.nanolett.0c03481.

Experimental methods, including supplementary discussion and figures (PDF)

https://dx.doi.org/10.1021/acs.nanolett.0c03481
Nano Lett. XXXX, XXX, XXX−XXX

Supplementary Movie 1 (AVI)

Supplementary Movie 2 (AVI)

AUTHOR INFORMATION

Corresponding Author

Kenneth L. Knappenberger Jr − *Department of Chemistry and Materials Research Institute, The Pennsylvania State University, University Park, Pennsylvania 16802, United States;* orcid.org/0000-0003-4123-3663; Email: klk260@psu.edu

Authors

Megan A. Steves − *Department of Chemistry, The Pennsylvania State University, University Park, Pennsylvania 16802, United States;* orcid.org/0000-0002-1410-5650

Yuanxi Wang − *Department of Physics and 2D Crystal Consortium, The Pennsylvania State University, University Park, Pennsylvania 16802, United States;* orcid.org/0000-0002-0659-1134

Natalie Briggs − *Department of Materials Science and Engineering, Materials Research Institute, and Center for 2D and Layered Materials, The Pennsylvania State University, University Park, Pennsylvania 16802, United States*

Tian Zhao − *Department of Chemistry, The Pennsylvania State University, University Park, Pennsylvania 16802, United States*

Hesham El-Sherif − *Department of Materials Science and Engineering, McMaster University, Hamilton, ON L8S 4L8, Canada; Mechanical Design and Production Engineering Department, Cairo University, Giza 12613, Egypt*

Brian M. Bersch − *Department of Materials Science and Engineering, Materials Research Institute, and Center for 2D and Layered Materials, The Pennsylvania State University, University Park, Pennsylvania 16802, United States*

Shruti Subramanian − *Department of Materials Science and Engineering, Materials Research Institute, and Center for 2D and Layered Materials, The Pennsylvania State University, University Park, Pennsylvania 16802, United States;* orcid.org/0000-0002-8933-9486

Chengye Dong − *Materials Research Institute and Center for 2D and Layered Materials, The Pennsylvania State University, University Park, Pennsylvania 16802, United States*

Timothy Bowen − *Department of Materials Science and Engineering, Materials Research Institute, and Center for 2D and Layered Materials, The Pennsylvania State University, University Park, Pennsylvania 16802, United States*

Ana De La Fuente Duran − *Department of Materials Science and Engineering, The Pennsylvania State University, University Park, Pennsylvania 16802, United States*

Katharina Nisi − *Walter Schottky Institute, Technical University of Munich, 85748 Garching, Germany*

Margaux Lassaunière − *Institute of Physics, University of Münster, 48149 Münster, Germany*

Ursula Wurstbauer − *Institute of Physics, University of Münster, 48149 Münster, Germany*

Nabil D. Bassim − *Department of Materials Science and Engineering, McMaster University, Hamilton, ON L8S 4L8, Canada*

Jose Fonseca − *U.S. Naval Research Laboratory, Washington, DC 20375, United States*

Jeremy T. Robinson − *U.S. Naval Research Laboratory, Washington, DC 20375, United States;* orcid.org/0000-0001-8702-2680

Vincent H. Crespi − *Department of Physics and 2D Crystal Consortium, The Pennsylvania State University, University Park, Pennsylvania 16802, United States*

Joshua Robinson − *2D Crystal Consortium, Department of Materials Science and Engineering, Materials Research Institute, and Center for 2D and Layered Materials, The Pennsylvania State University, University Park, Pennsylvania 16802, United States*

Complete contact information is available at: https://pubs.acs.org/10.1021/acs.nanolett.0c03481

Author Contributions

The manuscript was written through contributions of all authors. All authors have given approval to the final version of the manuscript.

Notes

The authors declare no competing financial interest.

ACKNOWLEDGMENTS

This research was supported by the Air Force Office of Scientific Research, grant number FA-9550-18-1-0347, and by the National Science Foundation Graduate Research Fellowship Program under grant no. DGE1255832. This work was also supported by the National Science Foundation, award number CHE-1807999 and under NSF DMR-2011839 through the Penn State MRSEC−Center for Nanoscale Science. Funding for this work was also provided by the Northrop Grumman Mission Systems' University Research Program, Semiconductor Research Corporation Intel/Global Research Collaboration Fellowship Program, task 2741.001, the National Science Foundation (NSF) CAREER Awards 1453924 and 1847811, the Chinese Scholarship Council, an Alfred P. Sloan Research Fellowship, the NSF DMR-1708972, DMR-1420620, and 1808900, and the 2D Crystal Consortium NSF Materials Innovation Platform under cooperative agreement DMR-1539916. Funding for the McMaster work was by AFOSR award FA9550-19-1-0239 and the NSERC Natural Sciences and Engineering Research Council of Canada Discovery Grant program. All electron microscopy was performed at the Canadian Centre for Electron Microscopy. The work at NRL was funded through the Office of Naval Research.

REFERENCES

(1) Li, G.; Zhang, S.; Zentgraf, T. Nonlinear Photonic Metasurfaces. *Nature Reviews Materials* **2017**, *2*, 17010.

(2) Capasso, F.; Sirtori, C.; Cho, A. Y. Coupled Quantum Well Semiconductors with Giant Electric Field Tunable Nonlinear Optical Properties in the Infrared. *IEEE J. Quantum Electron.* **1994**, *30* (5), 1313−1326.

(3) Janisch, C.; Wang, Y.; Ma, D.; Mehta, N.; Elías, A. L.; Perea-López, N.; Terrones, M.; Crespi, V.; Liu, Z. Extraordinary Second Harmonic Generation in Tungsten Disulfide Monolayers. *Sci. Rep.* **2015**, *4*, 1 DOI: 10.1038/srep05530.

(4) Janisch, C.; Song, H.; Zhou, C.; Lin, Z.; Elías, A. L.; Ji, D.; Terrones, M.; Gan, Q.; Liu, Z. MoS_2 Monolayers on Nanocavities: Enhancement in Light-Matter Interaction. *2D Mater.* **2016**, *3* (2), 025017.

(5) Seyler, K. L.; Schaibley, J. R.; Gong, P.; Rivera, P.; Jones, A. M.; Wu, S.; Yan, J.; Mandrus, D. G.; Yao, W.; Xu, X. Electrical Control of Second-Harmonic Generation in a WSe_2 Monolayer Transistor. *Nat. Nanotechnol.* **2015**, *10* (5), 407−411.

(6) Wu, F.; Tian, W.; Zhang, J.; Wang, S.; Wan, Q. X.; Dai, J. N.; Wu, Z. H.; Xu, J. T.; Li, X. Y.; Fang, Y. Y.; Chen, C. Q. Double-

Resonance Enhanced Intersubband Second-Order Nonlinear Optical Susceptibilities in GaN/AlGaN Step Quantum Wells. *Opt. Express* **2014**, *22* (12), 14212.
(7) Rosencher, E.; Fiore, A.; Vinter, B.; Berger, V.; Bois, P.; Nagle, J. Quantum Engineering of Optical Nonlinearities. *Science (Washington, DC, U. S.)* **1996**, *271* (5246), 168−173.
(8) Knippels, G. M. H.; van der Meer, A. F. G.; MacLeod, A. M.; Yelisseyev, A.; Isaenko, L.; Lobanov, S.; Thénot, I.; Zondy, J.-J. Mid-Infrared (275−60-Mm) Second-Harmonic Generation in LiInS_2. *Opt. Lett.* **2001**, *26* (9), 617.
(9) Lee, J.; Tymchenko, M.; Argyropoulos, C.; Chen, P. Y.; Lu, F.; Demmerle, F.; Boehm, G.; Amann, M. C.; Alù, A.; Belkin, M. A. Giant Nonlinear Response from Plasmonic Metasurfaces Coupled to Intersubband Transitions. *Nature* **2014**, *511* (7507), 65−69.
(10) Clark, D. J.; Senthilkumar, V.; Le, C. T.; Weerawarne, D. L.; Shim, B.; Jang, J. I.; Shim, J. H.; Cho, J.; Sim, Y.; Seong, M. J.; Rhim, S. H.; Freeman, A. J.; Chung, K. H.; Kim, Y. S. Strong Optical Nonlinearity of CVD-Grown MoS_2 Monolayer as Probed by Wavelength-Dependent Second-Harmonic Generation. *Phys. Rev. B: Condens. Matter Mater. Phys.* **2014**, *90* (12), 121409.
(11) Briggs, N.; Bersch, B.; Wang, Y.; Jiang, J.; Koch, R. J.; Nayir, N.; Wang, K.; Kolmer, M.; Ko, W.; De La Fuente Duran, A.; Subramanian, S.; Dong, C.; Shallenberger, J.; Fu, M.; Zou, Q.; Chuang, Y.-W.; Gai, Z.; Li, A.-P.; Bostwick, A.; Jozwiak, C.; Chang, C.-Z.; Rotenberg, E.; Zhu, J.; van Duin, A. C. T.; Crespi, V.; Robinson, J. Atomically Thin, Half-van Der Waals Metals Enabled by Confinement Heteroepitaxy. *Nat. Mater.* **2020**, *19*, 637.
(12) Zhao, T.; Jarrett, J. W.; Johnson, J. S.; Park, K.; Vaia, R. A.; Knappenberger, K. L. Plasmon Dephasing in Gold Nanorods Studied Using Single-Nanoparticle Interferometric Nonlinear Optical Microscopy. *J. Phys. Chem. C* **2016**, *120* (7), 4071−4079.
(13) Jarrett, J. W.; Zhao, T.; Johnson, J. S.; Knappenberger, K. L. Investigating Plasmonic Structure-Dependent Light Amplification and Electronic Dynamics Using Advances in Nonlinear Optical Microscopy. *J. Phys. Chem. C* **2015**, *119* (28), 15779−15800.
(14) Chang, L.; Pfeiffer, M. H. P.; Volet, N.; Zervas, M.; Peters, J. D.; Manganelli, C. L.; Stanton, E. J.; Li, Y.; Kippenberg, T. J.; Bowers, J. E. Heterogeneous Integration of Lithium Niobate and Silicon Nitride Waveguides for Wafer-Scale Photonic Integrated Circuits on Silicon. *Opt. Lett.* **2017**, *42* (4), 803.
(15) Attaccalite, C.; Palummo, M.; Cannuccia, E.; Grüning, M. Second-Harmonic Generation in Single-Layer Monochalcogenides: A Response from First-Principles Real-Time Simulations. *Phys. Rev. Mater.* **2019**, *3*, 74003.
(16) Jackson, A. G.; Ohmer, M. C.; LeClair, S. R. Relationship of the Second Order Nonlinear Optical Coefficient to Energy Gap in Inorganic Non-Centrosymmetric Crystals. *Infrared Phys. Technol.* **1997**, *38* (4), 233−244.
(17) Krause, D.; Teplin, C. W.; Rogers, C. T. Optical Surface Second Harmonic Measurements of Isotropic Thin-Film Metals: Gold, Silver, Copper, Aluminum, and Tantalum. *J. Appl. Phys.* **2004**, *96* (7), 3626−3634.
(18) Liebsch, A. *Electronic Excitations at Metal Surfaces* **1997**, 1.
(19) Petukhov, A. V.; Liebsch, A. Surface Anisotropy in Optical Second Harmonic Generation. I. Al(111). *Surf. Sci.* **1995**, *334* (1−3), 195−208.
(20) Lu, A.-Y.; Zhu, H.; Xiao, J.; Chuu, C.-P.; Han, Y.; Chiu, M.-H.; Cheng, C.-C.; Yang, C.-W.; Wei, K.-H.; Yang, Y.; Wang, Y.; Sokaras, D.; Nordlund, D.; Yang, P.; Muller, D. A.; Chou, M.-Y.; Zhang, X.; Li, L.-J. Janus Monolayers of Transition Metal Dichalcogenides. *Nat. Nanotechnol.* **2017**, *12* (8), 744−749.
(21) Kochat, V.; Samanta, A.; Zhang, Y.; Bhowmick, S.; Manimunda, P.; Asif, S. A. S.; Stender, A. S.; Vajtai, R.; Singh, A. K.; Tiwary, C. S.; Ajayan, P. M. Atomically Thin Gallium Layers from Solid-Melt Exfoliation. *Sci. Adv.* **2018**, *4* (3), e1701373.
(22) Heinz, T. F. Second-Order Nonlinear Optical Effects at Surfaces and Interfaces. In *Nonlinear Surface Electromagnetic Phenomena*; Ponath, H.-E., Stegeman, G. I., Eds.; Elsevier: 1991; pp 353−416.
(23) Shen, Y. Optical Second Harmonic Generation At Interfaces. *Annu. Rev. Phys. Chem.* **1989**, *40* (1), 327−350.

https://dx.doi.org/10.1021/acs.nanolett.0c03481
Nano Lett. XXXX, XXX, XXX−XXX